

PIV and UDM measurement of axial and circumferential flow modes between rotating disks

Masato Furue, Jiro Funaki and Katsuya Hirata
Dept. Mech. Eng., Doshisha Univ., Kyoto, 610-321, Japan

In the present study, we experimentally investigate the flow between co-rotating disks in a stationary cylindrical enclosure. This flow is often non-axisymmetrical and complicated. This flow sometimes causes magnetic-head oscillations in disks storage devices of PCs. We carry out the measurements of radial velocities by UDM (Ultrasonic Doppler Method) analyses, as well as flow visualizations using a high-speed camera and PIV (Particle Image Velocimetry) analyses. Tested cases are two, that is, A ($Re=1.22 \times 10^4$ and $\delta=0.12$) and B ($Re=2.44 \times 10^4$ and $\delta=0.20$). Here, Re is the rotating Reynolds number, and δ is a non-dimensional gap between disks. Case A is in the axial mode and Case B is in the axial mode. Here, the axial modes are related with the symmetry of a pair of toroidal-vortical structures. As a result, in case A, non-dimensional dominant frequency is about 20 from radial velocity, while half of 20 from axial velocity. In case B, non-dimensional dominant frequency is much lower than near 20, which is considered to be related with the circumferential mode.

Keywords: Co-rotating disks, Flow visualization, PIV, UDM

1 INTRODUCTION

Our present interest is the flow between two disks. Namely, we consider a pair of the same radius in a stationary cylindrical enclosure. The gap between disks is much narrower than the disk's radius. The disks are connected with a common shaft and co-rotate. Such a flow is often seen in hard-disk drives, the most popular storage devices in modern PCs. This flow is often complicated and non-axisymmetrical, consisting of two regions, that is, the core region in solid-body rotation and the outer turbulent region. The flow causes pressure and velocity fluctuations, and yields read/write errors of hard-disk drives due to magnetic-head oscillation. Therefore, for the accurate positioning operation of read/write magnetic heads in high-speed and high-capacity hard-disk drives, we are required to understand the flow.^[1]

Until now, various researches have been carried out in order to know the flow. Lennemann (1974) observed some non-axisymmetric circumferential modes.^[2] We can usually observe that two flow regions, namely, the core region in solid body rotation near the centre shaft, and the outer turbulent region. There is almost rigid-body-rotational flow in the core region, and much larger velocity fluctuation in outer turbulent region. The core region has a polygonally-shaped boundary, and the polygonal shape rotates slower than disks. Lenneman defined the circumferential mode with the number of core apices. In the outer turbulent region, flow is not completely turbulent, but has a larger structures described below. Later, Herrero et al. (1999) performed three-dimensional numerical simulations for the flow between co-rotating disks, and classified the flow into three axial modes, and .^[3] We can usually observe a pair of toroidal-

vortical structures near the stationary cylindrical enclosure in the outer turbulent region. In the axial mode, the vortical structures are steady and keep symmetry with respect to the interdisk midplane. In the axial mode, the symmetry is broken with a periodic fluctuation. In the axial mode, the symmetry is broken in a random manner without periodicity. For a need to comprehend the flow field between co-rotating disks from three-dimensional point of view, we (2005) have conducted an experimental study using quasi-three-dimensional PIV (Particle Image Velocimetry) analysis technique based on time-successive real-time analysis.^[1]

In the present study, we conduct radial velocity measurements based on UDM (Ultrasonic Doppler Method) technique. As well, we carry out flow visualizations by high-speed camera and time-successive three-dimensional PIV analyses. Our purpose is to get accurate and precise information in order to reveal the complicated flow with both axial and circumferential modes. More concretely, we study two cases with the axial modes and .

2 EXPERIMENTAL METHOD

2.1 Apparatus and governing parameters

Fig.1 shows a schematic diagram of our experimental apparatus. The experimental apparatus is a geometrically-simplified model of hard-disk drives. Two disks with the same radius are connected with a common shaft. Variable-speed motor makes the shaft rotate. The working fluid is water with which we fill the stationary cylindrical enclosure including two disks. The gap between disks is controlled by inserting acrylic pipes between disks as a spacer. Pipes are painted black in order to prevent the reflection of a YAG laser.

The present coordinate system is cylindrical (r, θ ,

z). Important geometrical parameters are as follows (see Fig.1). Disk radius R_d ($=153$ [mm]), acrylic-pipe radius R_s ($=34$ [mm]) and stationary-cylindrical enclosure radius R_w ($=155$ [mm]) is fixed to be constant. The gap between disks is G .

Rotating Reynolds number based on the disk radius is

$$Re = \frac{\omega R_d^2}{\nu} \tag{1}$$

Here, ν is the coefficient of kinematic viscosity. ω is disk-rotation speed, and is fixed to 5[rpm] or 10[rpm]. Corresponding Re is 1.22×10^4 and 2.44×10^4 .

The aspect ratio of disk gap to disk radius is

$$\delta = \frac{G}{R_d} \tag{2}$$

δ is equal to 0.12 or 0.20. Non-dimensional radius of the stationary cylindrical enclosure is

$$\lambda = \frac{R_w}{R_d} \tag{3}$$

As the gap between a disk tip and a stationary cylindrical enclosure is sufficiently narrow ($0.013R_d$), λ is approximately 1.0.

Tab.1 shows the details of our experimental parameters. We performed experiments for two cases; namely, Case A and Case B, which are in the axial mode, and in the axial mode, respectively. The velocity scale is the disk tip velocity V_d and the scale time is one period of the disk rotation t_d .

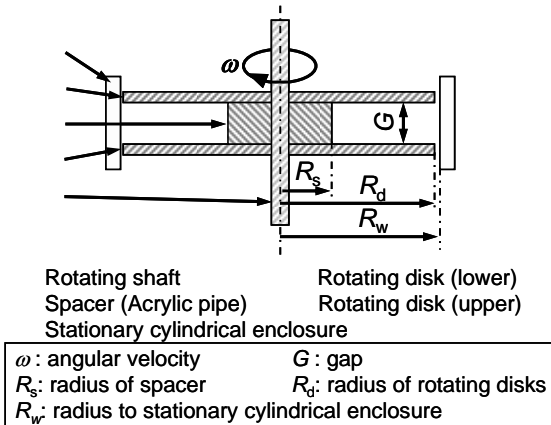


Fig.1 : Schematic diagram of model.

Tab.1 : Experimental parameters.

Case	A	B
Axial modes		
Circumferncial modes	more than 6	
Re	1.22×10^4	2.44×10^4
δ	0.12	0.20
λ	1.0	1.0

2.2 Classification of axial modes and circumferncial modes

2.2.1 Axial modes

We can usually observe a pair of toroidal-vortical structures near the stationary cylindrical enclosure in the outer turbulent region (see later). On the basis of the vortical structure's stability, Herrero et al.^[3] classified the flow into three, namely, axial modes, and. In the mode, the vortical structures are steady and keep symmetry with respect to the interdisk midplane. In the mode, the symmetry is broken with a periodic fluctuation. In the mode, the symmetry is broken in random manner without periodicity.

2.2.2 Circumferncial modes

When we observe the flow on the $r-\theta$ plane, we can usually observe that there are two flow regions; namely, the core region in solid-body rotation near the centre shaft, and the outer turbulent region. These regions are well characterized by radial profiles of circumferncial velocity^[4]. We can confirm almost rigid-body-rotation flow with very small velocity fluctuation in the core region, and non-rigid-body-rotation flow with much larger velocity fluctuation in outer turbulent region.

The core region has a polygonally-shaped boundary, and the polygonal shape rotates a little bit slower than disks. Lenneman^[2] defined the circumferncial mode with the number of core apices. For example, in the circumferncial mode 3, we see a triangle of the solid-body rotation core region. In addition, in the outer turbulent region, flow is not completely turbulent, but has large vortical structures in the circumferncial plane as well as the axial plane.

2.3 UDM Measurement

We conduct to measurements of radial velocity v_r . The tracer particle is chemically-briged polyethylene-resion particles coated with fluorescent paint and less than 100[μ m] of diameter. Ultrasonic inflects by the stationary cylindrical enclosure. In order to remove the inflection, we cut a part of cylindrical enclosure to make flat plane in the outside of cylindrical enclosure.

2.4 Flow visualization and PIV analysis

We also conduct both flow visualization and PIV analyses. The flow visualizations are performed using the same particles as the UDM measurements. For the PIV analyses, we use two consecutive photos, and carry out cross-correlation analyses. A laser sheet from a YAG laser lightens up the $r-z$ plane or the $r-\theta$ plane between two of disks. The flow visualization is recorded by a high-speed camera. Light inflection through the stationary cylindrical enclosure induces the distortion of images. In order to remove the distortion, we put a square-prism container surrounding the cylindrical enclosure, and fill up water between the cylindrical

enclosure and the square-prism container.

3 RESULTS AND DISCUSSION

3.1 Case A (axial mode)

Fig.2 shows PIV analyses on the r - z plane. Five successive figures (a)-(e) are taken with a regular interval of the same non-dimensional time t/t_d of 0.100/4. We can see a pair of toroidal-vortical structures near the cylindrical enclosure. The structures fluctuate periodically in the z direction. Then we can classify the flow into the mode . Note that the core boundary is at $r/R_d = 0.65$, and that the fluctuation of v_r is much smaller than v_z far from the core boundary.

Fig.3 (a) shows the time history of radial velocity v_r by PIV, and Fig.3 (b) shows one by UDM. The vertical axis is non-dimensionalised as v_r/V_d and horizontal axis is non-dimensionalised as t/t_d . The measuring point is non-dimensional radius $r/R_d=0.93$ and on the interdisk midplane. Fig.4 shows the spectral analyses of the fluctuating component of Fig.3, respectively. There is one dominant spectral peak at non-dimensional frequency ($f \cdot t_d$) of 20.8 by PIV, and at ($f \cdot t_d$) of 20.7 by UDM. Therefore, we can confirm a good agreement between PIV and UDM, and the accuracy of PIV.

Fig.5 (a) shows the time history of axial velocity v_z by PIV, and Fig.5 (b) shows spectral analysis of it. In Fig.5, the measuring point is same as Fig.3. We can confirm the one dominant peak in Fig.5 (b). However, the peak is about 9.97, which is half of Fig.4 because of the singularity of the interdisk midplane.

3.2 Case B (axial mode)

Fig.6 shows PIV analyses on the r - z plane. Five successive figures (a)-(e) are taken with a regular interval of the same non-dimensional time t/t_d of 0.333/4. We can see a pair of toroidal-vortical structures near the cylindrical enclosure. The structures are not symmetry and fluctuate non-periodically in the z direction. Then we can classify the flow into mode .

Fig.7 (a) shows the time history of v_r by PIV, and Fig.7 (b) shows one by UDM. The measuring point is same as Fig.3. Fig.8 shows the spectral analyses of Fig.7, respectively. There is one dominant spectral peak at ($f \cdot t_d$) of 1.99 by PIV, and at ($f \cdot t_d$) of 2.00 by UDM. Again, we can confirm a good agreement between PIV and UDM, and the accuracy of PIV.

Fig.9 (a) shows the time history of v_z by PIV, and Fig.9 (b) shows the spectral analysis of it. Also, the measuring point is the same as Fig.7. We can confirm one dominant spectral at ($f \cdot t_d$) of 2.99, no dominant peaks at ($f \cdot t_d$) 20. Hence, the dominant peaks are considered to corresponding to the circumferential mode 2 or 3.

4 CONCLUSIONS

In order to reveal the flow modes between co-rotating disks, we have conducted both PIV and UDM measurements for two cases A and B. The following conclusions are obtained.

1. We have confirmed the axial modes (Case A) and (Case B), using UDM measurement technology, as well as PIV analysis. Both results by UDM and PIV show good agreements, by which we can confirm the accuracy of PIV.
2. In the axial mode (Case A), radial velocity shows dominant non-dimensional frequency of 21. In particular, axial velocity on the interdisk midplane shows half of this frequency.
3. In axial mode , both radial and axial velocities show no dominant spectrum peak at non-dimensional frequency of about 20, but show a dominant peak at much lower frequency. The peak is considered to correspond to the circumferential mode 2 or 3.

REFERENCES

- [1] Hirata K, Furue M, Sugawara N, Funaki J: An experimental study of three-dimensional vortical structures between co-rotating disks, IOP Journal of Physics Conference Series, Vol.14 (2005), 213-219.
- [2] Lennemann E: Aerodynamic aspects of disk files, IBM J. Res. Dev., Vol.15, No.16 (1974) 480-488.
- [3] Herrero J, Giralt F, Humphery J A C: Influence of the geometry on the structure of the flow between a pair of corotating disks, Physics of Fluids, Vol.11, No.1 (1999) 88-96.
- [4] Funaki J, Takizawa K, Hirata K, Yano H: Flow modes in gap between coaxial rotating disks, Trans.JSME, Vol.61, No.588 (1995) 160-165 (in Japanese).

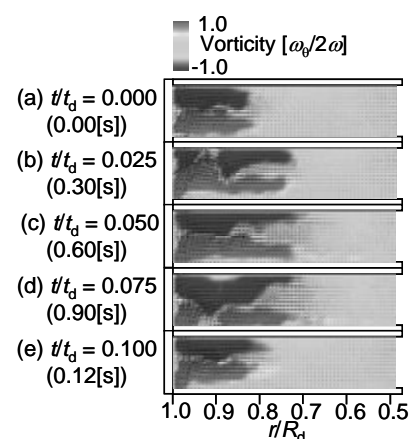


Fig.2 : Velocity vectors and vorticity ω_b on the r - z plane (for Case A).

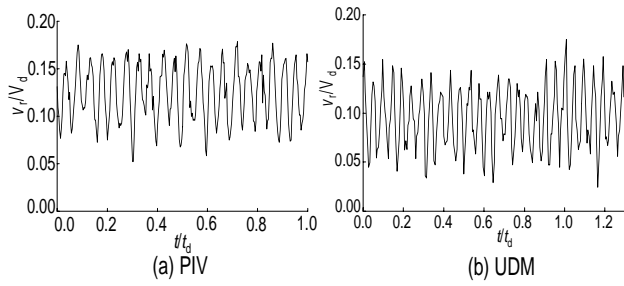


Fig.3 : Radial velocity v_r at $r/R_d=0.93$ and on the interdisk midplane (for Case A).

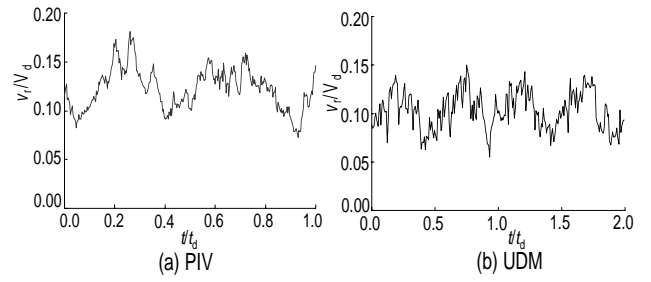


Fig.7 : Radial velocity v_r at $r/R_d=0.93$ and on the interdisk midplane (for Case B).

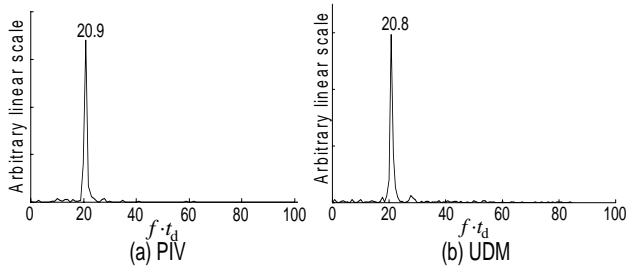


Fig.4 : Spectra of radial velocity v_r at $r/R_d=0.93$ and on the interdisk midplane (for Case A).

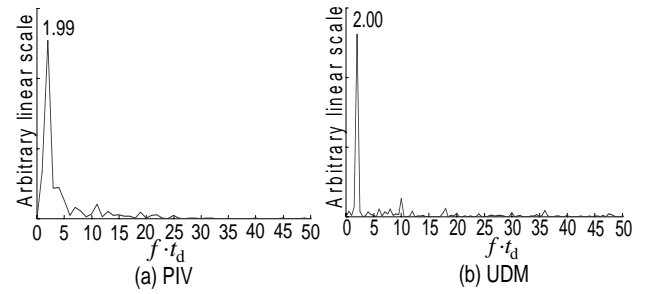


Fig.8 : Spectra of radial velocity v_r at $r/R_d=0.93$ and on the interdisk midplane (for Case B).

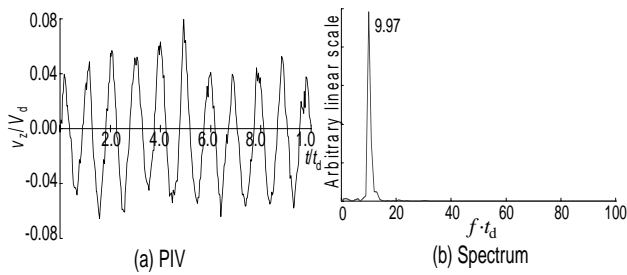


Fig.5 : Axial velocity v_z (by PIV) at $r/R_d=0.93$ on the interdisk midplane, and its spectrum (for Case A).

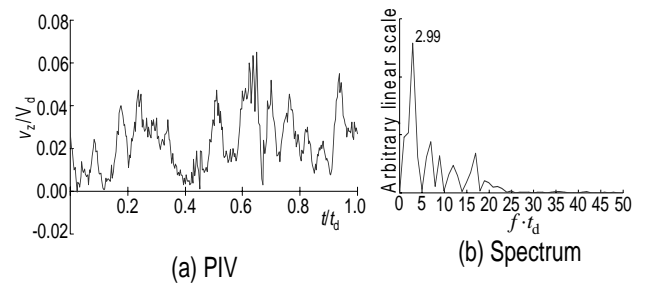


Fig.9 : Axial velocity v_z (by PIV) at $r/R_d=0.93$ on the interdisk midplane, and its spectrum (for Case B).

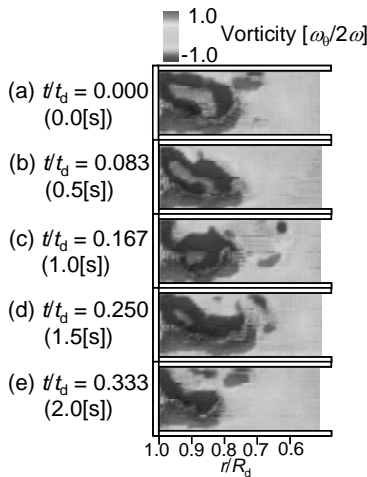


Fig.6 : Velocity vectors and vorticity α_θ at $r/R_d=0.93$ and on the interdisk midplane (for Case B).